Unusual Dynamics of Concentration Fluctuations in Solutions of Weakly Attractive Globular Proteins – Supporting Information

Saskia Bucciarelli,[†] Lucía Casal-Dujat,[†] Cristiano De Michele,[‡] Francesco Sciortino,[‡,¶] Jan Dhont,[§,‖] Johan Bergenholtz,[⊥,†] Bela Farago,[#] Peter Schurtenberger,[†] and Anna Stradner[*,†]

Physical Chemistry, Department of Chemistry, Lund University, SE-22100 Lund, Sweden, Department of Physics, Università di Roma La Sapienza, I-00186 Roma, Italy, CNR-ISC Uos, Università di Roma La Sapienza, I-00186 Roma, Italy, Forschungszentrum Jülich, Institute of Complex Systems (ICS), Soft Condensed Matter (ICS-3), D-52425 Jülich, Germany, Heinrich-Heine-Universität Düsseldorf, Department of Physics, D-40225 Düsseldorf, Germany, Department of Chemistry and Molecular Biology, University of Gothenburg, SE-41296, Göteborg, Sweden, and Institut Laue-Langevin, F-38042 Grenoble Cedex 9, France

E-mail: Anna.Stradner@fkem1.lu.se

[*]To whom correspondence should be addressed
[†]Lund University
[‡]Università di Roma La Sapienza
[¶]CNR-ISC Uos
[§]Forschungszentrum Jülich
[‖]Heinrich-Heine-Universität Düsseldorf
[⊥]University of Gothenburg
[#]ILL

Sample preparation

Bovine γ_B-crystallin was isolated and purified from nuclear portions of calf lenses, obtained fresh as a by-product from a local slaughterhouse, using size exclusion chromatography (Superdex 200 prep grade) with a 275 mM Na-acetate buffer at pH 4.5, followed by a cation exchange column (SP Sepharose Fast Flow), using 275 mM Na-acetate buffer, pH 4.8, and a 0-325 mM NaCl gradient to elute the protein.[1] After purification, the buffer had to be exchanged to the final solvent, a 52.4 mM phosphate buffer in 100% D_2O at pH 7.1 (close to the pI of γ_B[2]), containing 20 mM DTT to prevent oxidation of the proteins and 0.02 wt% NaN_3 to prevent bacterial growth. The pH and ionic strength of the buffer are chosen to mimic physiological conditions, while the use of D_2O instead of H_2O as solvent is required to minimize the incoherent background contribution in the Neutron Spin Echo experiments. Moreover, heavy water as solvent increases the critical temperature of the liquid-liquid phase separation as compared to H_2O and thus shifts the phase transitions into an experimentally accessible temperature range. Buffer exchange and subsequent sample concentration was done by ultrafiltration using Amicon centrifugal filter units with a cut-off of 3K. The concentration of the final protein solutions was determined by UV absorption spectroscopy at a wavelength of $\lambda = 280$ nm, using the specific absorption coefficient $E^{1\%,280\text{nm}}_{\gamma_B,1\text{cm}} = 2.18$ ml/mg·cm.[1] The protein concentration c was converted to volume fraction ϕ using $\phi = c \cdot v$, where $v = 0.7$ ml/g is the protein voluminosity.[3]

Static light scattering (SLS) experiments

Light scattering experiments and transmission measurements were performed on either a homebuilt multi-angle instrument[4] or a commercial goniometer system (3D LS Spectrometer, LS Instruments AG). Both instruments implement the so-called 3D cross-correlation technique to suppress contributions from multiple scattering, essential for measurements in the vicinity of a critical point or spinodal line.[5] The q-range covered by LS is 0.001-0.003 $Å^{-1}$, where the scattering vector

$q = [4\pi n(\sin\theta/2)]/\lambda$ depends on the scattering angle θ, the refractive index n of the solution and the wavelength λ. We did not find any q-dependence of the scattered intensity within the range covered by LS. The values measured at different scattering angles θ were thus simply averaged to yield the singly scattered intensity. $S(0)$ was then derived directly from the average of the scattered intensity, after background correction and normalization with concentration and a measurement of a very dilute sample (form factor). Moreover, all SLS measurements were corrected for multiple scattering following established procedures for the employed 3D cross-correlation technique.[5] The lowest volume fractions were however only measured at $\theta = 90^\circ$ and $S(0)$ derived from the average of multiple measurements.

In order to determine the cloud point, the transmission of protein samples at varying ϕ was monitored while the temperature was gradually lowered, starting at 308 K, until the sample became highly turbid, marking the onset of liquid-liquid phase separation. We used a previously established protocol where the temperature at which the transmission dropped to half of its initial value was used as the cloud point T_{cloud}.[6] Shallow quenches to temperatures T just below the critical temperature T_c lead to liquid-liquid phase separation and after complete demixing into two transparent phases, the concentration of the dilute phase was determined and used to complete the low-ϕ branch of the binodal, as described by Thurston[1]. SLS at different θ was used to determine the spinodal. Linear extrapolation of the singly scattered intensity as a function of T yields an estimate of the spinodal temperature T_{sp}.[7]

Small-angle X-ray scattering (SAXS) experiments

SAXS measurements were performed on a pinhole camera (Ganesha 300 XL, SAXSLAB), equipped with a high brilliance microfocus sealed tube, a Pilatus detector and a thermostated sample stage. The detector is mounted on a motor, allowing to move it over 1400 mm, thus changing the sample-

detector distance and leading to a large accessible q-range (0.003-2.5 Å^{-1}). Every measurement was corrected for background radiation, transmission, buffer and capillary and normalized with the protein concentration c. This concentration-normalized scattering intensity can be expressed as $I(q)/c \sim P(q)S(q)$, with $S(q)$ being the static structure factor and $P(q)$ the form factor. The latter was determined at low concentration where $S(q) \approx 1$ and thus $P(q) = I_0(q)/c_0$ where $I_0(q)$ is the measured intensity of the dilute sample with concentration c_0. The structure factors of more concentrated samples are then given by $S(q) = [I(q)/c]/P(q)$.

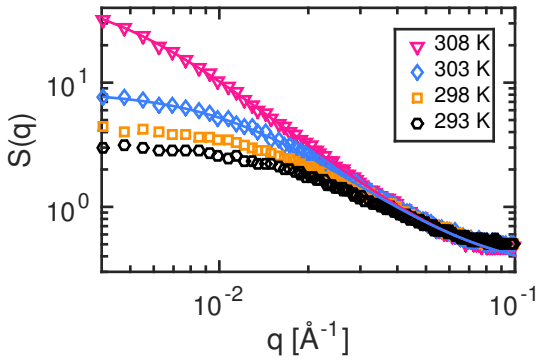

Figure S1: SAXS $S(q)$ (symbols) as a function of T for $\phi = 0.16$ (close to ϕ_c) and the corresponding OZ fits (lines).

Examples of the resulting $S(q)$ for a sample close to the critical volume fraction ϕ_c are given in Figure S1. We analyze the total scattering of the proteins $S(q,T,\phi) = \left[S_{\text{crit}}(0)/\left(1+q^2\xi_s^2\right)\right] + S_{\text{non-crit}}(\phi)$ as a sum of a non-critical background ($S_{\text{non-crit}}(\phi)$) and a strongly temperature-dependent critical component ($\left[S_{\text{crit}}(0)/\left(1+q^2\xi_s^2\right)\right]$) given by the Ornstein-Zernike (OZ) equation. Here the temperature dependence of $S_{\text{crit}}(0)$ and ξ_s are given by $S_{\text{crit}}(0) = S_0\tau^{-\gamma}$ and $\xi_s = \xi_{s,0}\tau^{-\nu}$, where $\nu = 0.63$ and $\gamma = 1.24$ are the corresponding critical exponents from the Ising universality class,[8,9] $\tau = \left(T - T_{\text{sp}}\right)/T_{\text{sp}}$ is the reduced temperature and $S_{\text{non-crit}}$ accounts for the (small) non-critical component, assumed to be q-independent in the low-q regime ($q \ll q^*$) considered here.[10] Using S_0, $\xi_{s,0}$, T_{sp} and $S_{\text{non-crit}}$ as fit parameters and simultaneously fitting the structure factors at all measured T close to criticality (lines in Figure S1), we find that $\xi_{s,0} = (7.27 \pm 0.71)$ nm and that T_{sp} from SAXS closely follows the spinodal determined by cloud point measurements. The total forward scattering intensity $S(0) = S_{\text{crit}}(0) + S_{\text{non-crit}}$, directly related to the osmotic compressibility κ_T, is

shown in Figure 2a of the main manuscript (open symbols).

Dynamic light scattering (DLS) experiments

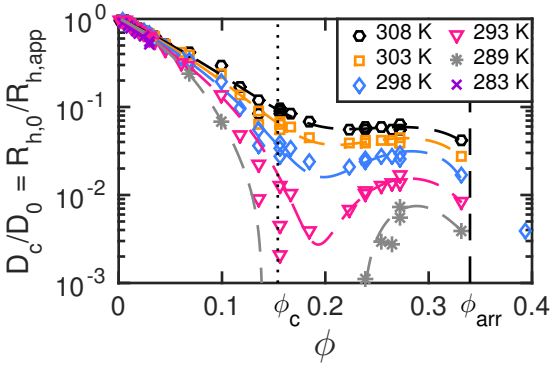

Figure S2: Normalized D_c from DLS versus ϕ as a function of T. The dashed lines serve as guides to the eye. The vertical dotted and dashed black lines mark the critical concentration ϕ_c and the arrest concentration ϕ_{arr}, respectively.

When performing DLS experiments close to a critical point or spinodal, it is essential to suppress contributions from multiple scattering, which can easily be done by utilizing a so-called 3D cross-correlation technique.[5] From the measured intensity cross-correlation functions we first calculated the field correlation function or intermediate scattering function ISF, and then obtained the collective diffusion coefficient D_c from the initial decay of the ISF. The resulting normalized diffusion coefficients D_c/D_0, where $D_0 = k_B T/[6\pi\eta(T)R_{h,0}]$ is the free diffusion coefficient of a non-interacting γ_B-crystallin with $R_{h,0} = 2.27$ nm, are shown as a function of volume fraction and temperature for all samples measured in Figure S2. This quantity corresponds to the normalized apparent hydrodynamic radius $R_{h,app}/R_{h,0}$ or normalized dynamic correlation length $\xi_d/\xi_{d,0}$. The dashed lines connecting the individual data points for a single temperature are replotted in Figure 2b in the main manuscript.

We in addition performed DLS experiments in order to establish the arrest line above the binodal also shown in Figure 1 of the main manuscript. Here we rely on the fact that the measured correlation functions clearly exhibit characteristic changes when the sample undergoes a transi-

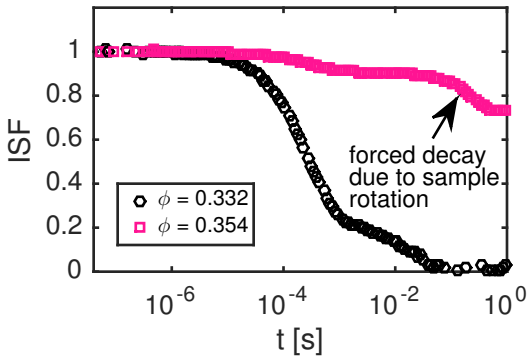

Figure S3: Intermediate scattering functions at 308 K just below ($\phi = 0.332$, ○) and above ($\phi = 0.354$, □) the glass transition, measured at $\theta = 120°$. The non-ergodic sample was rotated at a speed of 0.04 rpm, causing the second, forced decay of the correlation function.

tion from ergodic to non-ergodic when crossing the arrest line. While ergodic samples result in correlation functions with a well-defined baseline and fully decay over the accessible time window, correlation functions obtained with solid-like or non-ergodic samples exhibit large variations in signal-to-baseline ratio and a non-decaying plateau that corresponds to the arrested motion of particles on long time scales in glassy samples. These samples also require a different sampling scheme in order to ensure a properly ensemble-averaged correlation function. We have chosen measurements where the sample cell is slowly rotated in order to create a forced slow decay of the arrested plateau and an appropriately averaged correlation function. Examples of correlation functions measured in the fluid ($\phi = 0.332$) and arrested ($\phi = 0.354$) state are shown in Figure S3 for a temperature of $T = 308$ K.

Neutron spin echo (NSE) experiments

NSE experiments were carried out on IN15 at ILL probing a q-range from 0.01 to 0.23 Å^{-1} and a Fourier time range between 0.03 and 600 nanoseconds. In this Letter, for the analysis of the NSE data, we focus on measurements performed at $q = q^* = 0.2$ Å^{-1}, where q^* closely corresponds to the nearest-neighbor peak in the structure factor of γ_B-crystallin solutions. A selection of ISFs measured by NSE is shown in Figure S4.

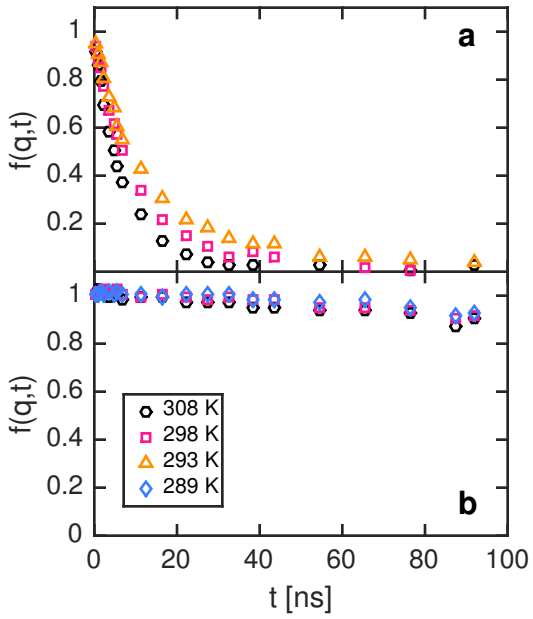

Figure S4: ISFs from NSE at different T for $\phi =$ (a) 0.10 and (b) 0.35.

Square-Well Hard Ellipsoid Model

The isothermal compressibility plot in Figure 2a of the main manuscript has been obtained for a monodisperse system of hard ellipsoids complemented with a square-well (SW) potential. The hard ellipsoids (HE) have semi-axes $a = 2.75$ nm, $b = 1.625$ nm and $c = 1.375$ nm and the SW attraction is defined as follows: given the two HEs A and B shown in Figure S5, consider the outer HEs A' and B' (transparent ones) of semi-axes $a+\Delta$, $b+\Delta$ and $c+\Delta$ (where $\Delta = 0.6$ nm), then the A and B interaction energy is 0 if A' and B' do now overlap or is $-\varepsilon$ if they do (see Figure S5).

Monte Carlo Simulations

Successive Umbrella Sampling (SUS) Monte Carlo (MC) simulations[11] in a cubic box with periodic boundary conditions have been used to calculate the equation of state for several temperatures. From a SUS simulation, the probability distribution $W[n]$ of observing n particles in the simulation box at fixed temperature T and chemical potential can be obtained.[11] Indeed, a SUS simulation consists in performing grand canonical simulations in parallel on many different systems where

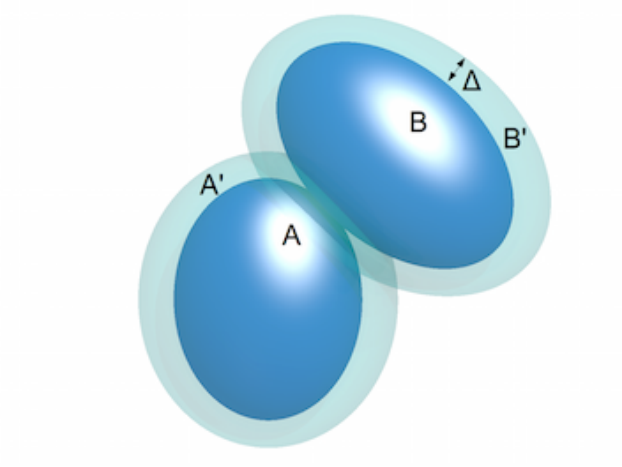

Figure S5: SWHE model: A and B are two hard ellipsoids complemented with a square-well interaction whose range is Δ.

the number of particles N ranges from 0 to N_m. The number of particles of system k is constrained within a window of size w_k, (in our case we chose $w_k = 2$ for all k) and consecutive windows overlap by one particle, i.e. if w_k ranges from n to $n+1$, then w_{k+1} ranges from $n+1$ to $n+2$. We denote by $H_k[n]$ the frequency that state n of kth windows is visited and H_{kl} and H_{kr} the histogram of its left and right boundary, respectively. The unnormalized probability distribution $W[n]$ is then given by:

$$\frac{W[n]}{W[0]} = \frac{H_{0r}}{H_{0l}} \cdot \frac{H_{1r}}{H_{1l}} \cdot \frac{H_{2r}}{H_{2l}} \cdots \frac{H_k[n]}{H_{kl}}. \tag{1}$$

The equation of state is obtained by calculating P and the number density ρ for different values of z from the following equations:

$$P(z,V,T) = \frac{1}{\beta V} \log\left(\frac{zV \sum_{n=0}^{N_m} W[n]}{W[1]}\right) \tag{2}$$

$$\rho(z,V,T) = \langle N/V \rangle = \frac{\sum_{n=0}^{N_m} (n/V) W[n]}{\sum_{n=0}^{N_m} W[n]} \tag{3}$$

where $\beta = 1/(k_B T)$, $\mathcal{Q}(z,V,T)$ is the grand partition function. The expressions for P and ρ in eqs. (Eq. (1)) and (Eq. (1)) depend on the probability distribution $W[n]$. The calculation of $W[n]$ for different values of z can be performed by histogram reweighting, which relies on the use of the following relation between the probability distribution at two different activities z and z':

$$\begin{aligned}\frac{W[n,z']}{W[n,z]} &= \frac{z'^n Q_n(V,T)}{\mathcal{Q}(z',V,T)} \cdot \frac{\mathcal{Q}(z,V,T)}{z^n Q_n(V,T)} \\ &= k\left(\frac{z'}{z}\right)^n \end{aligned} \tag{4}$$

where $Q_n(V,T)$ is the canonical partition function for a system of n particles and $k = \mathcal{Q}(z,V,T)/\mathcal{Q}(z',V,T)$, which does not depend on n, is just a normalization factor.

From the equation of state, the isothermal compressibility κ_T can be calculated using the following thermodynamic relation:

$$\kappa_T = \frac{\langle n^2 \rangle - \langle n \rangle^2}{\langle n \rangle \rho k_B T} \tag{5}$$

where $\langle \ldots \rangle$ represents an average over $W[n]$.

References

(1) Thurston, G. M. Liquid-Liquid Phase Separation and Static Light Scattering of Concentrated Ternary Mixtures of Bovine α and γB Crystallins. *J. Chem. Phys.* **2006**, *124*, 134909.

(2) Bloemendal, H.; de Jong, W.; Jaenicke, R.; Lubsen, N. H.; Slingsby, C.; Tardieu, A. Ageing and Vision: Structure, Stability and Function of Lens Crystallins. *Prog. Biophys. Mol. Biol.* **2004**, *86*, 407–485.

(3) Schurtenberger, P.; Chamberlin, R. A.; Thurston, G. M.; Thomson, J. A.; Benedek, G. B. Observation of Critical Phenomena in a Protein-Water Solution. *Phys. Rev. Lett.* **1989**, *63*, 2064–2067.

(4) Moitzi, C.; Vavrin, R.; Kumar Bhat, S.; Stradner, A.; Schurtenberger, P. A New Instrument for Time-Resolved Static and Dynamic Light-Scattering Experiments in Turbid Media. *J. Colloid Interface Sci.* **2009**, *336*, 565–574.

(5) Urban, C.; Schurtenberger, P. Characterization of Turbid Colloidal Suspensions Using Light Scattering Techniques Combined with Cross-Correlation Methods. *J. Colloid Interface Sci.* **1998**, *207*, 150–158.

(6) Asherie, N. Protein Crystallization and Phase Diagrams. *Methods* **2004**, *34*, 266–272.

(7) Thomson, J. A.; Schurtenberger, P.; Thurston, G. M.; Benedek, G. B. Binary Liquid Phase Separation and Critical Phenomena in a Protein/Water Solution. *Proc. Natl. Acad. Sci. U. S. A.* **1987**, *84*, 7079–7083.

(8) Kleinert, H. Critical Exponents from Seven-Loop Strong-Coupling φ^4 Theory in Three Dimensions. *Phys. Rev. D* **1999**, *60*, 085001.

(9) Pelissetto, A.; Vicari, E. Critical Phenomena and Renormalization-Group Theory. *Phys. Rep.* **2002**, *368*, 549–727.

(10) Biffi, S.; Cerbino, R.; Bomboi, F.; Paraboschi, E. M.; Asselta, R.; Sciortino, F.; Bellini, T. Phase Behavior and Critical Activated Dynamics of Limited-Valence DNA Nanostars. *Proc. Natl. Acad. Sci. U. S. A.* **2013**, *110*, 15633–15637.

(11) Virnau, P.; Muller, M. Calculation of Free Energy Through Successive Umbrella Sampling. *J. Chem. Phys.* **2004**, *120*, 10925–10930.